

Poisson to GOE transition in the distribution of ratio of consecutive level spacings

N. D. Chavda¹, H. N. Deota¹ and V. K. B. Kota²

¹*Applied Physics Department, Faculty of Technology and Engineering,*

M. S. University of Baroda, Vadodara 390 001, India

²*Physical Research Laboratory, Ahmedabad 380 009, India*

(Dated: October 28, 2018)

Abstract

Probability distribution for the ratio (r) of consecutive level spacings of the eigenvalues of a Poisson (generating regular spectra) spectrum and that of a GOE random matrix ensemble are given recently. Going beyond these, for the ensemble generated by the Hamiltonian $H_\lambda = (H^0 + \lambda V)/\sqrt{1 + \lambda^2}$ interpolating Poisson ($\lambda = 0$) and GOE ($\lambda \rightarrow \infty$) we have analyzed the transition curves for $\langle r \rangle$ and $\langle \tilde{r} \rangle$ as λ changes from 0 to ∞ ; $\tilde{r} = \min(r, 1/r)$. Here, V is a GOE ensemble of real symmetric $d \times d$ matrices and H^0 is a diagonal matrix with a Gaussian distribution (with mean equal to zero) for the diagonal matrix elements; spectral variance generated by H_0 is assumed to be same as the one generated by V . Varying d from 300 to 1000, it is shown that the transition parameter is $\Lambda \sim \lambda^2 d$, i.e. the $\langle r \rangle$ vs λ (similarly for $\langle \tilde{r} \rangle$ vs λ) curves for different d 's merge to a single curve when this is considered as a function of Λ . Numerically, it is also found that this transition curve generates a mapping to a 3×3 Poisson to GOE random matrix ensemble. Example for Poisson to GOE transition from a one dimensional interacting spin-1/2 chain is presented.

PACS numbers: 05.45.+b, 05.45.Mt, 75.10.Jm

I. INTRODUCTION

Energy level fluctuations in quantum systems whose classical analogue is chaotic will follow one of the three classical ensembles, the Gaussian orthogonal (GOE), unitary (GUE) or symplectic (GSE) ensemble depending on the symmetries of the Hamiltonian [1]. The nearest neighbor spacing distribution (NNSD) $P(S)dS$ giving degree of level repulsion is one of the commonly used measure for level statistics. More importantly Berry and Tabor [2] established that, if a quantum system is in integrable domain, corresponding to the regular behavior of the system, generically NNSD follows Poisson distribution [$P(S) = \exp(-S)$]. However, if the system is chaotic, as conjectured by Bohigas et al [3], NNSD is (for Hamiltonian preserving time-reversal and rotational invariance) described by the Wigner surmise which is essentially the GOE result [$P(S) = (\pi/2)S \exp(-\pi S^2/4)$].

Recently, the distribution $P(r)$ of the ratio (r) of consecutive level spacings of the energy levels and related averages (for example $\langle r \rangle$), which require no unfolding as they are independent of the form of the density of the energy levels, are established to be useful statistical measures to distinguish order from chaos in energy levels. The $P(r)$ and $\langle r \rangle$ will allow for a more transparent comparison with experimental results than the traditional NNSD. These are used to investigate numerically many-body localization in mesoscopic systems [4–7], to quantify the distance from integrability on finite size lattices appropriate for ultra cold atomic gases [8, 9], and also to establish, using embedded random matrix ensembles, that finite many particle quantum systems with strong enough interactions follow GOE [10]. Recently they are also used in the study of spectral correlations in diffuse van der Waals clusters [11]

Most of the many-particle quantum systems such as atoms, nuclei, quantum dots, small metallic grains and so on are mixed systems with level fluctuations intermediate to Poisson and GOE (in this paper we will restrict to systems with time reversal and rotational symmetry). In order to quantify the degree of chaos in a complex system, random matrix ensembles interpolating Poisson and GOE have been considered (see for example [1, 12–14]) and formulas for NNSD are derived. One of the most popular formula is the Brody distribution [15] and other that is used in deciding the Poisson to GOE transition marker is derived using a 2×2 interpolating matrix ensemble [16]. As the $P(r)$ distribution is established to be much better measure of level fluctuations than NNSD, it is important to study Poisson

to GOE transition in $P(r)$ for a random matrix ensemble that interpolates the two limiting distributions. In [10], a simple interpolation formulas was suggested by analogy with the Brody distribution. However, it is possible to write many more interpolating formulas. Because of this, it is important to derive $P(r)$ and related averages using a random matrix ensemble that interpolate the two limits. The purpose of the present paper is to address this problem and present some results. Now we will give a preview.

In Section II, to get started, analytical results for Poisson and GOE for the probability distribution $P(r)$ of the ratio of consecutive level spacings and related averages $\langle r \rangle$ and $\langle \tilde{r} \rangle$ (\tilde{r} is defined in Section II) are briefly discussed. Then, introduced is a 3×3 interpolating random matrix ensemble $\{H_\lambda\}$ giving Poisson and GOE at the limits. In Section III, a more general interpolating ensemble $\{H_\lambda\}$ for $d \times d$ matrices is introduced and using 1000 member ensembles with $d \leq 1000$, numerically studied are $\langle r \rangle$ and $\langle \tilde{r} \rangle$ as a function of the λ parameter. Established here are (i) the transition parameter $\Lambda \sim \lambda^2 d$ giving scaling, (ii) the universal form for the transition curves $\langle r \rangle, \langle \tilde{r} \rangle$ vs Λ and (iii) a map between $d \times d$ and 3×3 matrix ensembles. Section IV gives as a simple application of the transition curves, results for Poisson to GOE transition in a one dimensional interacting spin-1/2 chain. Finally, Section V gives conclusions and future outlook.

II. POISSON AND GOE FORMULAS FOR $P(r)$ AND A 3×3 ENSEMBLE FOR POISSON TO GOE TRANSITION

Let us consider an ordered set of eigenvalues (energy levels) E_n , where $n = 1, 2, \dots, d$. The nearest-neighbor spacing is given by $s_n = E_{n+1} - E_n$. Then, the ratio of two consecutive level spacings is $r_n = s_{n+1}/s_n$. The probability distribution for consecutive level spacings is denoted by $P(r)dr$. If the system is in integrable domain, nearest spacings follow Poisson and then $P(r)$ is [denoted by $P_P(r)$],

$$P_P(r) = \frac{1}{(1+r)^2}. \quad (1)$$

Similarly, for GOE, derived using 3×3 real symmetric matrices, the $P(r)$ is given by a Wigner-like surmise [17],

$$P_W(r) = \frac{27}{8} \frac{r+r^2}{(1+r+r^2)^{5/2}}. \quad (2)$$

In addition to r_n , it is possible to consider the distribution of the ratios \tilde{r}_n where $\tilde{r}_n = \frac{\min(s_n, s_{n-1})}{\max(s_n, s_{n-1})} = \min(r_n, 1/r_n)$. As pointed out in [17], it is possible to write down $P(\tilde{r})$ for given $P(r)$. In practice, besides $P(r)$, it is also useful to consider $\langle r \rangle$, the average value of r and $\langle \tilde{r} \rangle$, average value of \tilde{r} . For GOE, $\langle r \rangle = 1.75$ and for Poisson it is ∞ . Similarly, $\langle \tilde{r} \rangle = 0.536$ for GOE and 0.386 for Poisson. We will use $P(r)$, $\langle r \rangle$ and $\langle \tilde{r} \rangle$ in the following discussion.

For Poisson to GOE transition in NNSD a simple 2×2 ensemble was constructed in [18–20] and it was shown that the results of this ensemble can be mapped to those of any $d \times d$ matrix. Following this, it is possible to identify a 3×3 ensemble for Poisson to GOE interpolation in $P(r)$ and the related averages. To this, we consider the following 3×3 matrix ensemble $H_{3 \times 3}$,

$$H_{3 \times 3} = \begin{bmatrix} A & B & C \\ B & D & E \\ C & E & F \end{bmatrix} = \begin{bmatrix} -pvx & 0 & 0 \\ 0 & 0 & 0 \\ 0 & 0 & pvy \end{bmatrix} + \lambda \begin{bmatrix} a & b & c \\ b & d & e \\ c & e & f \end{bmatrix}. \quad (3)$$

In Eq. (3), x and y are independent Poisson variables with average unity so that the joint probability distribution $P(x, y) dx dy = \exp -(x + y) dx dy$ with $0 \leq x, y \leq \infty$. Similarly, a , b , c , d , e and f are independent Gaussian variables with zero center and variance $2v^2$ for a , d and f [i.e. they are independent $G(0, 2v^2)$ variables] while it is v^2 for b , c and e [i.e. they are independent $G(0, v^2)$ variables]. Also, in Eq. (3) λ is a parameter and p is a constant introduced for convenience. In the limit $\lambda = 0$, $H_{3 \times 3}$ gives for $P(r)$ the Poisson result in Eq. (1). Similarly for $\lambda \rightarrow \infty$, $H_{3 \times 3}$ gives for $P(r)$ the GOE result in Eq. (2). Thus, as λ changes from 0 to ∞ , $H_{3 \times 3}$ generates Poisson to GOE transition in $P(r)$ and the related averages. Firstly it is easy to see that in the limit $\lambda = 0$, the average spacing between the nearest eigenvalues is $\overline{D}_0 = pv$. Now, the joint probability distribution for the matrix elements A, B, C, D, E and F of $H_{3 \times 3}$ is easy to write down. Say that the eigenvalues of H are E_i , $i = 1, 2$ and 3 and the orthogonal matrix that diagonalizes H is generated by three angles and say they are θ_i , $i = 1, 2$ and 3. Then, the joint distribution $\rho(A, B, C, D, E, F)$ in A, B, C, D, E and F is

$$\rho(A, B, C, D, E, F) = \mathcal{N} \exp - \left\{ \frac{(A + pvx)^2 + D^2 + (F - pvy)^2}{4\lambda^2 v^2} + \frac{B^2 + C^2 + E^2}{\lambda^2 v^2} \right\}$$

and $dAdBdCdDdEdF$ is of the form $\prod_{i < j} |E_i - E_j| f(\theta_1, \theta_2, \theta_3) dE_1 dE_2 dE_3 d\theta_1 d\theta_2 d\theta_3$. Note that \mathcal{N} is a normalization constant and the function $f(\theta_1, \theta_2, \theta_3)$ follows from the Jacobi

transformation from (A, B, C, D, E, F) to $(E_1, E_2, E_3, \theta_1, \theta_2, \theta_3)$. Putting $E_i = 2\lambda v x_i$, we have

$$\begin{aligned} & \rho(x_1, x_2, x_3, \theta_1, \theta_2, \theta_3) dx_1 dx_2 dx_3 d\theta_1 d\theta_2 d\theta_3 = \\ & \mathcal{N}' \exp - \left\{ \sum_{i=1}^3 x_i^2 + \frac{p^2 v^2}{4\lambda^2 v^2} (x^2 + y^2) + \frac{pv}{\lambda v} [x f_1(x_1, x_2, x_3, \theta_1, \theta_2, \theta_3) - y g_1(x_1, x_2, x_3, \theta_1, \theta_2, \theta_3)] \right\} \\ & \times \prod_{i < j} |x_i - x_j| f(\theta_1, \theta_2, \theta_3) dx_1 dx_2 dx_3 d\theta_1 d\theta_2 d\theta_3 \end{aligned} \quad (4)$$

Note that f_1 and g_1 in Eq. (4) transform A and F in Eq. (3) into x_i (i.e. E_i) and θ_i and \mathcal{N}' is a normalization constant. Integrating the R.H.S. of Eq. (4) over $(\theta_1, \theta_2, \theta_3)$ and also over x and y with the weight factor $P(x, y) = \exp -(x + y)$ will give $\rho(x_1, x_2, x_3)$ and there by $P(r)$. This problem, we could not solve so far. However, Eq. (4) gives the important result that $\rho(E_1, E_2, E_3)$ and therefore $P(r)$ will depend only the transition parameter Λ where

$$\Lambda = \frac{\lambda^2 v^2}{p^2 v^2} = \frac{\lambda^2 v^2}{[\overline{D_0}]^2}. \quad (5)$$

This is nothing but the square of the admixing matrix element divided by the average spacing between the unperturbed ($\lambda = 0$) levels. Now we will consider a general $d \times d$ matrix for Poisson to GOE transition and show that this ensemble can be mapped to the $H_{3 \times 3}$ ensemble.

III. A GENERAL $d \times d$ ENSEMBLE FOR POISSON TO GOE TRANSITION: NUMERICAL RESULTS

Following the work in [19], we will consider the interpolating Hamiltonian ensemble

$$H_\lambda = \frac{H_0 + \lambda V}{\sqrt{1 + \lambda^2}} \quad (6)$$

where H_0 is a diagonal matrix with $(H_0)_{ii}, i = 1, 2, \dots, d$ being independent $G(0,1)$ variables. Similarly V is chosen as a GOE with matrix elements variance v^2 (for diagonal matrix elements it is $2v^2$). Note that the spectral variance generated by H_0 is $\overline{\sigma^2(H_0)} = 1$ and the one generated by V is $\overline{\sigma^2(V)} = v^2(d + 1)$. We choose H_0 and V such that $\overline{\sigma^2(H_0)} = \overline{\sigma^2(V)}$ giving $v^2 \sim 1/d$ for large d . Similarly, as $\sigma(H_0) = 1$ we have $D_0 \sim 1/d\rho_0$. Here, ρ_0 is the eigenvalue density generated by H_0 . With these, for the H ensemble given by Eq. (6) the transition parameter is $\Lambda = \frac{\lambda^2 v^2}{[\overline{D_0}]^2} \sim \lambda^2 d \rho_0^2$. Replacing ρ_0 by its average value we have

$$\Lambda = \lambda^2 d / 2\pi \quad (7)$$

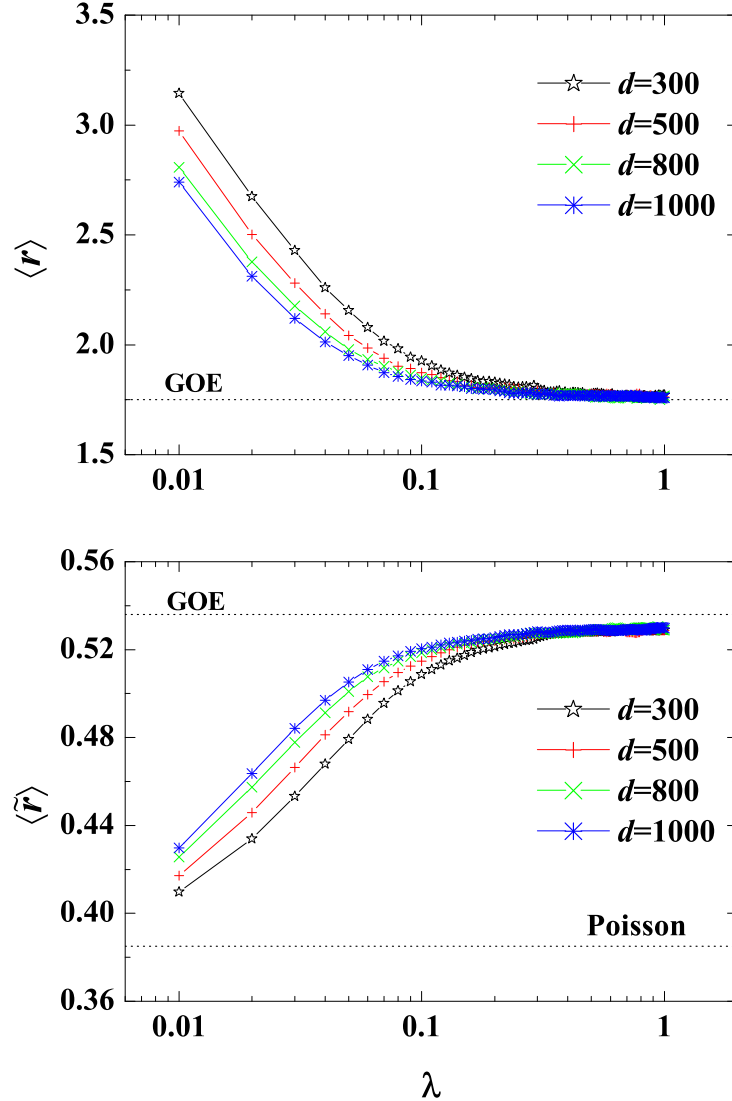


FIG. 1. (Color online) Variation of $\langle r \rangle$ (upper Panel) and $\langle \tilde{r} \rangle$ (lower panel) as a function of λ for $d \times d$ matrix ensembles defined by H_λ in Eq. (6). Results are shown for $d = 300 - 1000$ with 1000 member ensembles.

as the transition parameter. We will see ahead the significance of the Λ parameter in Eq. (7). As we do not have an analytical solution for $P(r)$ for the H_λ ensemble, we have undertaken large scale numerical investigation with matrix dimensions changing from 300 to 1000. Instead of studying the variation of the $P(r)$ function with λ for various values of d , we have considered $\langle r \rangle$ and $\langle \tilde{r} \rangle$ vs λ . Fig. 1 shows the results for d changing from 300 to 1000. As seen from the figures, the curves change with dimension d . Thus, the curves are

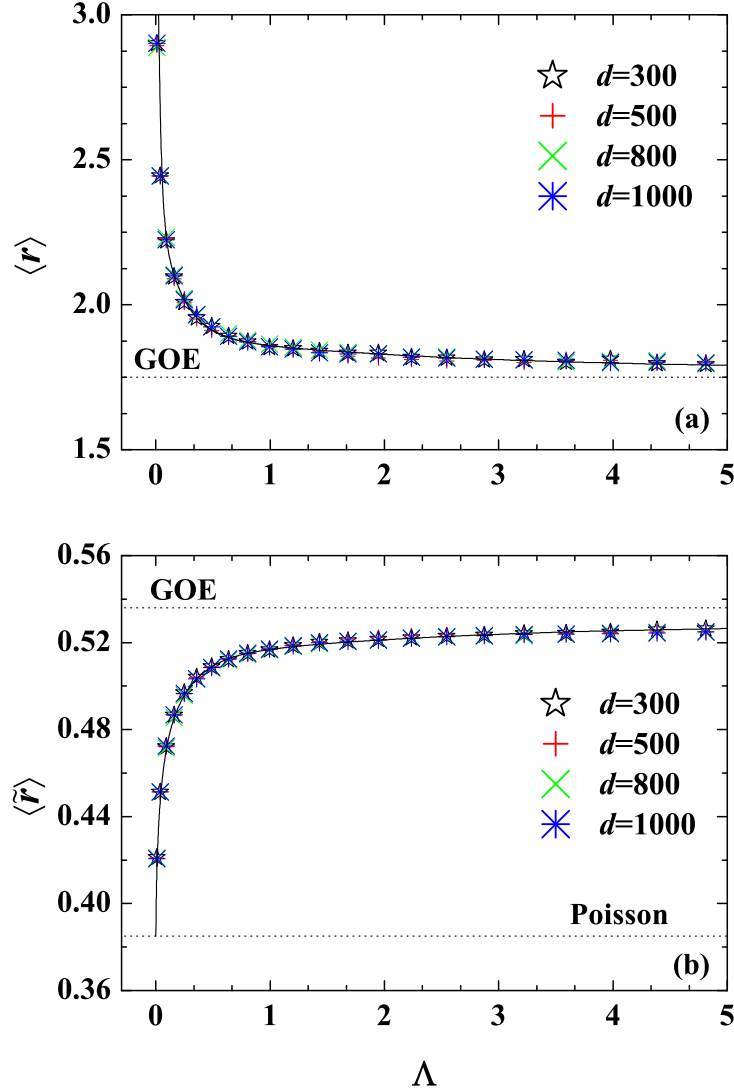


FIG. 2. (Color online) Same as Fig. 1 but for $\langle r \rangle$ (upper Panel) and $\langle \tilde{r} \rangle$ (lower panel) vs $\lambda^2 d$. The continuous curves represent the best fits to the results and these give the universal transition curves.

not universal when $\langle r \rangle$ and $\langle \tilde{r} \rangle$ and plotted against the λ parameter. However, as shown in Fig. 2 the curves will be independent of d when we use the transition parameter $\lambda^2 d \sim \Lambda$ given by Eq. (7). Thus, the curves given in Fig. 2 are universal curves.

It is possible to define a critical value Λ_c for the transition parameter Λ for Poisson to GOE transition that defines the onset of GOE fluctuations. As $\langle \tilde{r} \rangle$ changes from 0.386 to 0.536 with level fluctuations changing from Poisson to GOE, from Fig. 2b a good choice appears to be $\langle \tilde{r} \rangle = 0.5$ with $\Lambda_c \sim 0.3$. This condition gives from Fig. 2a that $\langle r \rangle = 2$

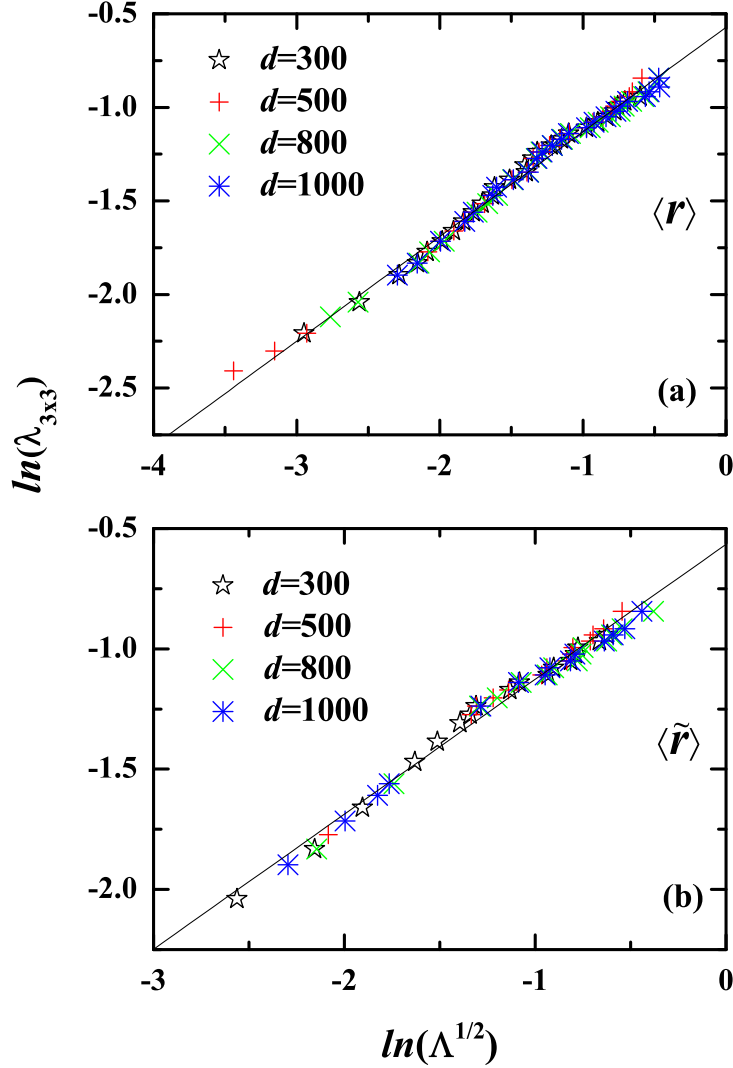


FIG. 3. (Color online) $\lambda_{3 \times 3}$ from 3×3 ensemble vs Λ from $d = 300$ to 1000. Upper panel gives the result obtained from $\langle r \rangle$ and the lower panel from $\langle \tilde{r} \rangle$. The straight lines are obtained via fitting linear relation to numerical results. See text for details.

for $\Lambda = \Lambda_c$. This criterion can be used to determine onset of chaos (GOE fluctuations) in complex many-body systems. Some examples will be discussed in Section IV.

Another important result is that there is a mapping between the 3×3 ensemble defined by Eq. (3) and $d \times d$ ensemble defined by Eq. (6). This is as follows. In order to avoid confusion between the λ used in Eq. (3) and Eq. (6), we denote the λ in $H_{3 \times 3}$ as $\lambda_{3 \times 3}$ from now onwards. Numerically, using 50000 members, the 3×3 ensemble defined by Eq. (3) was constructed and calculated are $\langle r \rangle$ and $\langle \tilde{r} \rangle$ as a function of $\lambda_{3 \times 3}$. Using these and the

results in Fig. 2, one can determine given a value of $\lambda_{3 \times 3}$, the value of Λ (for any d) that gives the same value for $\langle r \rangle$ and similarly $\langle \tilde{r} \rangle$. Plot of $\lambda_{3 \times 3}$ vs Λ thus determined using $\langle r \rangle$ is given in Fig. 3a. Similar plot obtained using $\langle \tilde{r} \rangle$ is given in Fig. 3b. It is clearly seen from Figs. 3a and 3b that the curves $\lambda_{3 \times 3}$ and Λ are linearly correlated. The straight lines, in Figs. 3a and 3b, are due to linear fit to $\langle r \rangle$ vs Λ and $\langle \tilde{r} \rangle$ vs Λ curves respectively. It is interesting to note that both the results give similar slope. Therefore the $\langle r \rangle$ vs Λ and $\langle \tilde{r} \rangle$ vs Λ transition curves can be derived by solving the 3×3 ensemble defined by Eq. (3) and this will be addressed in future.

IV. APPLICATIONS TO A DISORDERED INTERACTING SPIN-1/2 CHAIN

Chains of interacting spins-1/2 systems are prototype quantum many-body systems. They have been considered as models for quantum computers, magnetic compounds and have recently been simulated in optical lattices [21–23]. In the past, the transition from integrability to chaos was investigated for a Heisenberg spin-1/2 chain with defects using NNSD [24]. Here we will consider this model to display order to chaos transition using $P(r)$ distribution by varying the defect strength. The Hamiltonian describing the system of a spin-1/2 chain is

$$H = \sum_{n=1}^L \omega_n S_n^z + \varepsilon S_d^z + \sum_{n=1}^{L-1} J \hat{S}_n \cdot \hat{S}_{n+1}. \quad (8)$$

Here L is the number of sites and $\hbar = 1$. $\hat{S}_n = \vec{\sigma}_n/2$ are the spin operators at site n , and $\vec{\sigma}$ are the Pauli spin matrices. The first term in Eq. (8) corresponds to the Zeeman splitting of each spin n determined by the static magnetic field in the z -direction giving the energy splitting ω_n . If all sites are assumed to have same energy splitting ω except a single site d , where the splitting is $\omega + \varepsilon$ then this site is referred to as the defect (second term in Eq. (8)). If $\omega_n = \omega$ for all sites with $\varepsilon = 0$ then the chain is called clean. The last term in Eq. (8) describes two type of couplings between the nearest neighbor spins. First is the diagonal Ising interaction ($S_n^z S_{n+1}^z$) and second is off-diagonal flip-flop term ($S_n^x S_{n+1}^x + S_n^y S_{n+1}^y$). The later term is responsible for propagating the excitation through the chain. To avoid degeneracy found in the spectrum of a close chain (chain with periodic boundaries), in the present analysis we use an open chain (with free boundaries). Further more, we have considered isotropic chain, i.e. coupling strength between the Ising interaction is equal to that of the flip-flop term

and it is taken as constant. These one-dimensional systems of interacting spin-1/2 chain are devoid of random elements and involve only two-body interactions.

For the chain described by Eq. (8), the z component of the total spin $\sum_{n=1}^L S_n^z$ is conserved, so states with same number of excitations are coupled. Here the focus is on $L/2$ excitations giving largest number of states. In the absence of defects (when the chain is clean), spin-1/2 chain is integrable and is solved with the Bethe ansatz [25]. An open chain with defects only on the edges is also integrable [26]. NNSD for such an interacting chain follows Poisson distribution. On the other hand, when there is only one defect in the middle of the chain and the defect excess energy is of the order of the interaction strength then NNSD for such chain is described by Wigner-Dyson distribution [24]. When defect strength is very strong compared to that of interaction then an excitation on one side of the chain would not have enough energy to overcome the defect and reach the other side of the chain. In this situation, the chain said to be broken giving an integrable model and Poisson form for NNSD is recovered [24]. Here to display Poisson to GOE transition, the evolution of $P(r)$ is studied with respect to the defect strength with $\varepsilon \leq J$ and taking defect site at the middle of the chain with $d = L/2$.

Figure 4 represents $P(r)$ histograms constructed, using $L = 14$ sites and 7 excitations, for various values of ε . The dimensionality of the system is 3432. The figure clearly displays the transition of $P(r)$ from the Poisson character for low values of ε to the GOE character as the strength of the defect is slowly increased by increasing ε . The transition of $P(r)$ is smooth in character with respect to the parameter ε . Figure 5 shows variation of $\langle r \rangle$ and $\langle \tilde{r} \rangle$ as a function of parameter ε . The demarcation between the Poisson to GOE region giving critical value of defect strength, at which the transition is complete, is found to be $\varepsilon_c = \varepsilon(\langle \tilde{r} \rangle = 0.5) = 0.1$ for the example considered. It is striking that the figures in Fig. 5 are similar to those in Fig. 2 confirming that the random matrix model considered in Section III will be appropriate for the 1D spin-1/2 chain system with H defined by Eq. (8).

V. CONCLUSIONS

Going beyond the results presented in [10], studied is the Poisson to GOE transition in the distribution $P(r)$ of the ratio of consecutive level spacings and the related averages $\langle r \rangle$ and $\langle \tilde{r} \rangle$. Main conclusions are: (i) there is a scaling in $P(r)$, $\langle r \rangle$ and $\langle \tilde{r} \rangle$ measures similar to

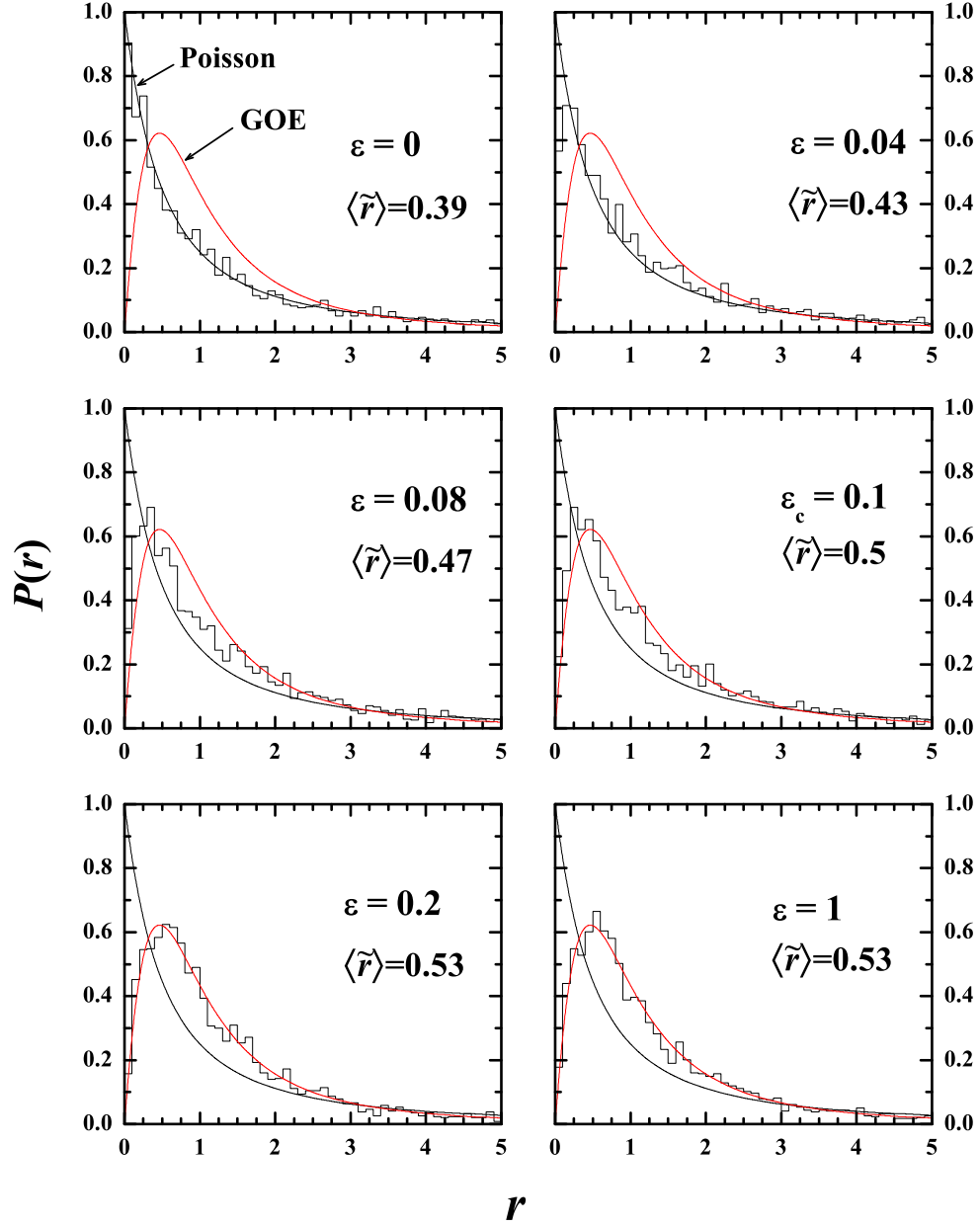


FIG. 4. (Color online) Histograms represent $P(r)$ distribution, for H in Eq. (8) with $L = 14$ with 7 excitations, for various values of defect strengths ε . The defect is on the site $d = 7$. In applying Eq. (8), the value of ω_n is chosen to be $\omega_n = 0$ for all n and similarly, J value is chosen to be $J = 1$. Values $\langle \tilde{r} \rangle$ are also given in the figure and $\langle \tilde{r} \rangle = 0.5$ gives value of chaos marker ε_c . Bin size equal to 0.1 is used for the histograms. The results are compared with Poisson and Wigner(GOE) predictions.

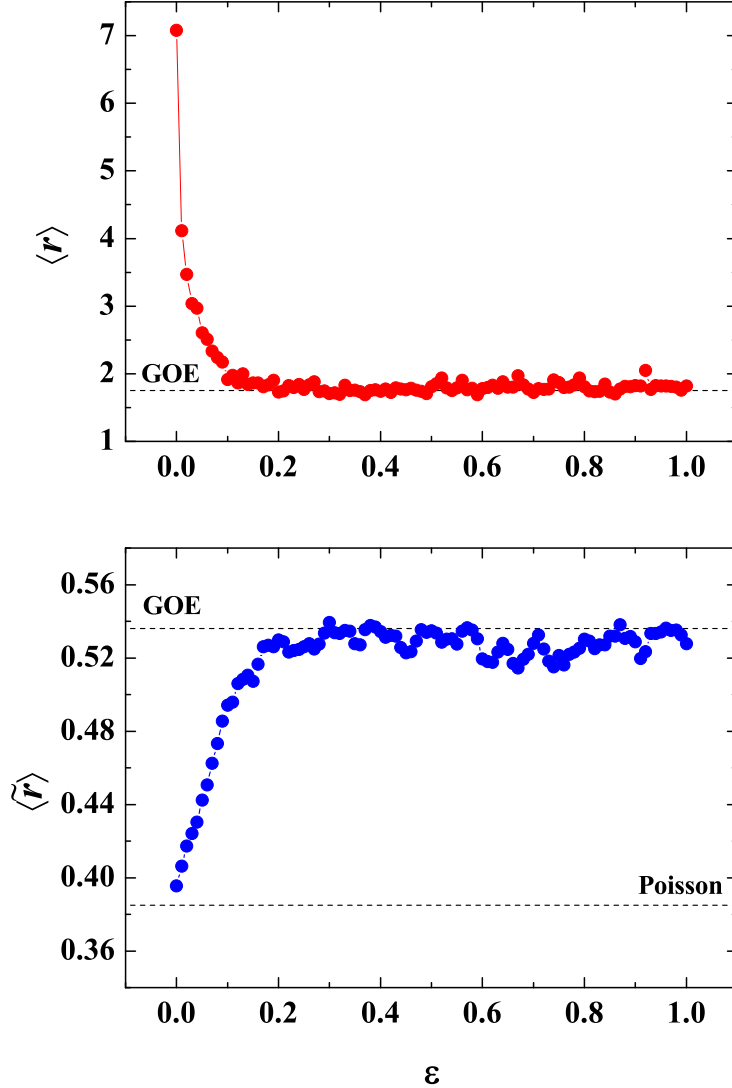


FIG. 5. (Color online) Average value of r_n (denoted as $\langle r \rangle$) (upper panel) and \tilde{r}_n (denoted as $\langle \tilde{r} \rangle$) (lower panel) as a function of defect strength ε for H in Eq. (8) with $L = 14$, 7 spins up and defect site $d = 7$.

the scaling seen before for NNSD and related averages such as the variance of NNSD giving a transition parameter Λ defined by Eq. (7); (ii) universal transition curves for $\langle r \rangle$ and $\langle \tilde{r} \rangle$ vs Λ are constructed numerically as given in Fig. 2; (iii) as seen from Fig. 3, the 3×3 random matrix ensemble given by Eq. (3) maps, for $P(r)$ and related averages, to the $d \times d$ matrices and this is similar to the mapping to a 2×2 matrix for NNSD [18–20]. As an example for Poisson to GOE transition in $P(r)$ and related averages, results for a one dimensional interacting spin-1/2 chain are presented. In future, it is important to solve analytically the

3×3 matrix ensemble defined by Eq. (3). Finally, the results presented in this paper should be useful in applications for systems discussed in [4–9, 27]

ACKNOWLEDGMENTS

We thank Soumik Bandyopadhyay for collaboration in the initial stages of this work. One of the authors (NDC) acknowledges support from University Grant Commission (UGC), India [grant No: F.40-425/2011(SR)]. HND acknowledges support from UGC, India for a research fellowship [grant No. F. 7-198/2007(BSR)].

-
- [1] F. Haake, *Quantum Signatures of Chaos*, Third edition (Springer-Verlag, Heidelberg, 2010).
 - [2] M. V. Berry, M. Tabor, Proc. Roy. Soc. (London) **A356** (1977) 375.
 - [3] O. Bohigas, M.-J. Giannoni, C. Schmit, Phys. Rev. Lett. **52** (1984) 1.
 - [4] V. Oganesyan and D. A. Huse, Phys. Rev. **B 75** (2007) 155111.
 - [5] V. Oganesyan, A. Pal, and D. A. Huse, Phys. Rev. **B 80** (2009) 115104.
 - [6] A. Pal and D. A. Huse, Phys. Rev. **B 82** (2010) 174411.
 - [7] S. Iyer, V. Oganesyan, G. Refael, and D. A. Huse, Phys. Rev. B **87**, 134202 (2013).
 - [8] C. Kollath, G. Roux, G. Biroli, and A. M. Läuchli, J. Stat. Mech. (2010) P08011.
 - [9] M. Collura, H. Aufderheide, G. Roux, and D. Karevski, Phys. Rev. **A 86** (2012) 013615.
 - [10] N.D. Chavda and V.K.B. Kota, Phys. Lett. A **377**, 3009 (2013).
 - [11] S.K. Haldar, B. Chakrabarti, N.D. Chavda, T.K. Das, S. Canuto, and V. K. B. Kota, Phys. Rev. A **89**, 043607 (2014).
 - [12] M.L. Mehta, *Random Matrices*, 3rd Edition, (Elsevier B.V., Netherlands, 2004).
 - [13] G. Akemann, J. Baik, P. Di Francesco (Editors), *The Oxford Handbook of Random Matrix Theory* (Oxford University Press, Oxford, 2011).
 - [14] V. K. B. Kota, Phys. Rep. **347** (2001) 223.
 - [15] T.A. Brody, Lett. Nuovo. Cim. **7**, 482 (1973).
 - [16] V.K.B. Kota, *Embedded Random Matrix Ensembles in Quantum Physics*, Lecture Notes in Physics, volume 884 (Springer, Heidelberg, 2014).
 - [17] Y. Y. Atas, E. Bogomolny, O. Giraud, and G. Roux, Phys. Rev. Lett. **110** (2013) 084101.

- [18] G. Lenz and F. Haake, Phys. Rev. Lett. **65**, 2325 (1991).
- [19] G. Lenz, K. Zyczkowski, and D. Saher, Phys. Rev. A **44**, 8043 (1991).
- [20] V.K.B. Kota and S. Sumedha, Phys. Rev. **E 60** (1999) 3405.
- [21] I. Bloch, J. Dalibard, W. Zwerger, Rev. Mod. Phys. **80** (2008) 885.
- [22] J. Simon, W. S. Bakr, R. Ma, M. E. Tai, P. M. Preiss, and M. Greiner, Nature **472** (2011) 307.
- [23] S. Trotzky, Yu-Ao Chen, A. Flesch, Ian P. McCulloch, U. Schollwck, J. Eisert, I. Bloch, Nature Physics **8** (2012) 325.
- [24] L. F. Santos, J. Phys. **A 37** (2004) 4723.
- [25] H. A. Bethe, Z. Phys. **71** (1931) 205.
- [26] F. C. Alcaraz, M. N. Barber, M. T. Batchelor, R. J. Baxter, and G. R. W. Quispel, J. Phys. **A 20** (1987) 6397.
- [27] E.J. Torres-Herrera and L.F. Santos, Phys. Rev. A **89** (2014) 043620.